

Enhancement and inverse behaviors of magnetoimpedance in a magnetotunneling junction by driving frequency

W. C. Chien, C. K. Lo, L. C. Hsieh, Y. D. Yao, X. F. Han, Z. M. Zeng, T. Y. Peng, and P. Lin

Citation: *Applied Physics Letters* **89**, 202515 (2006); doi: 10.1063/1.2374807

View online: <http://dx.doi.org/10.1063/1.2374807>

View Table of Contents: <http://scitation.aip.org/content/aip/journal/apl/89/20?ver=pdfcov>

Published by the [AIP Publishing](#)

Articles you may be interested in

[Improvement of the low-frequency sensitivity of MgO-based magnetic tunnel junctions by annealing](#)

J. Appl. Phys. **109**, 113917 (2011); 10.1063/1.3596817

[80% tunneling magnetoresistance at room temperature for thin Al-O barrier magnetic tunnel junction with CoFeB as free and reference layers](#)

J. Appl. Phys. **101**, 09B501 (2007); 10.1063/1.2696590

[Microstructure investigation on barrier shapes of double barrier magnetic tunnel junctions](#)

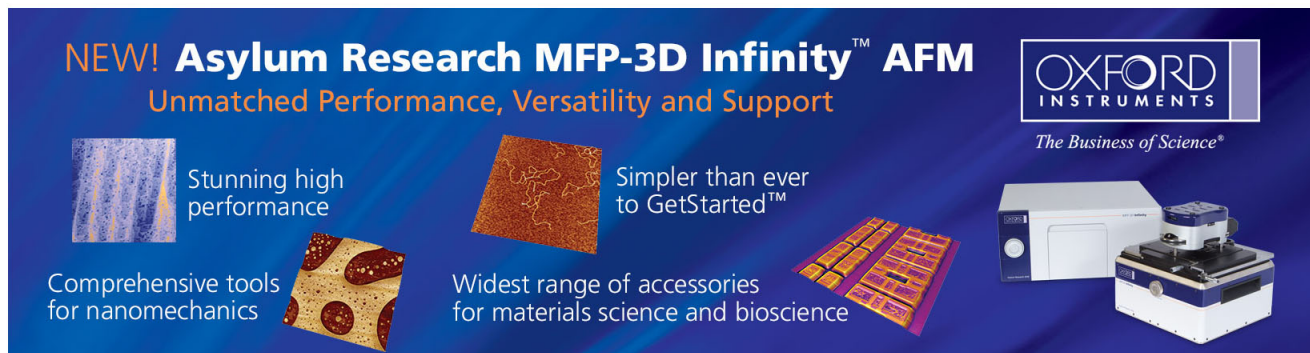
J. Appl. Phys. **100**, 054510 (2006); 10.1063/1.2337765

[Bias voltage dependence of magnetic tunnel junctions comprising double barriers and amorphous NiFeSiB layers](#)

J. Appl. Phys. **99**, 08A902 (2006); 10.1063/1.2165129

[Thermal stability of Ir - Mn Co - Fe - B Al - O Co - Fe - B tunnel junctions](#)

J. Appl. Phys. **98**, 113710 (2005); 10.1063/1.2137888



NEW! Asylum Research MFP-3D Infinity™ AFM
Unmatched Performance, Versatility and Support

OXFORD INSTRUMENTS
The Business of Science®

Stunning high performance

Simpler than ever to GetStarted™

Comprehensive tools for nanomechanics

Widest range of accessories for materials science and bioscience

Asylum Research

Enhancement and inverse behaviors of magnetoimpedance in a magnetotunneling junction by driving frequency

W. C. Chien

Department of Materials Science and Engineering, National Chiao Tung University, Hsinchu 310, Taiwan

C. K. Lo and L. C. Hsieh

Electronics and Optoelectronics Research Laboratories (EOL), Industrial Technology Research Institute, Hsinchu 310, Taiwan and Nano Technology Research Center, ITRI, Hsinchu 310, Taiwan

Y. D. Yao^{a)}

Division of Natural Science, Ming Hsin University of Science and Technology, Hsinchu 304, Taiwan and Institute of Physics, Academia Sinica, Taipei 115, Taiwan

X. F. Han and Z. M. Zeng

State Key Laboratory of Magnetism, Institute of Physics, Chinese Academy of Sciences, Beijing 100080, China and Beijing National Laboratory for Condensed Matter Physics, Institute of Physics, Chinese Academy of Sciences, Beijing 100080, China

T. Y. Peng and P. Lin

Department of Materials Science and Engineering, National Chiao Tung University, Hsinchu 310, Taiwan

(Received 12 July 2006; accepted 25 September 2006; published online 17 November 2006)

The magnetoimpedance effect was employed to study magnetotunneling junction (MTJ) with the structure of Ru(5 nm)/Cu(10 nm)/Ru(5 nm)/IrMn(10 nm)/CoFeB(4 nm)/Al(1.2 nm)-oxide/CoFeB(4 nm)/Ru(5 nm). A huge change of more than $\pm 17\,000\%$ was observed in the imaginary part of the impedance between the magnetically parallel and antiparallel states of the MTJ. The inverse behavior of the magnetoimpedance (MI) loop occurs beyond 21.1 MHz; however, the normal MI at low frequency and the inverse MI at high frequency exhibit the same magnetization reversal as checked by the Kerr effect. The reversal in MI was due to the dominance of magnetocapacitance at high frequency. © 2006 American Institute of Physics.

[DOI: 10.1063/1.2374807]

The magnetic tunnel junction (MTJ) is an excellent system for investigating the spin-polarized electron coherent tunneling effect and both theoretical and experimental studies on the MTJ are interesting topics of current research.^{1,2} However, the studies of impedance as a function of magnetic field on MTJ are still rare which motivated us to study the impedance as a function of magnetic fields on a MTJ system.

Inverse magnetoresistance (MR) behavior has been reported in the MTJ structure with a dc measurement,^{3,4} but the inverse magnetoimpedance (MZ) properties have not been studied yet. Most research on the hysteresis properties of MTJ focuses on dc measurement and low frequency ac measurement, which show low resistance in the parallel state and high resistance in the antiparallel state. In this study, the frequency was raised to 40 MHz, and the magnetoimpedance, $Z = |Z|e^{i\theta} = R + iX$ in which $X = X_L - X_C$,⁵⁻⁷ of a MTJ device was studied. The MZ ratio is defined as $100\% \times (Z_{AP} - Z_P)/Z_P$, where the subscript P (AP) stands for the parallel (antiparallel) magnetization orientation state of the MTJ.

The MTJ structures of Ru(5)/Cu(10)/Ru(5)/IrMn(10)/CoFeB(4)/Al(1.2)-oxide/CoFeB(4)/Ru(5) with dc-MR of 14.3% were deposited on Si/SiO wafers using the magnetron sputtering system, where all thicknesses are given in nanometers, with the junction area of $6 \times 6 \mu\text{m}^2$, as shown in Fig. 1. The ac behavior was determined by using the HP4194 impedance analyzer with the 16047D fixture. A two-point contact was used in a frequency range from

100 Hz to 40 MHz with a fixed oscillating voltage of 0.5 V, together with an electromagnet which supplied a dc field up to ± 500 Oe.

Figure 2 shows the frequency dependence of the real part of impedance (R_{AP}, R_P) and the imaginary part of impedance (X_{AP}, X_P) for the MTJ in the parallel and antiparallel states. The R_{AP} and R_P curves decrease with increasing frequency, which indicates that the MTJ includes a significant capacitance effect. Therefore, a Maxwell-Wagner model capacitor consisting of dielectric material⁸ with the equivalent

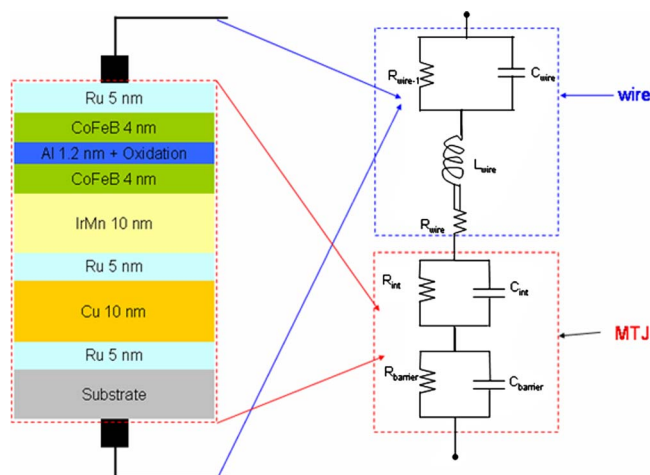


FIG. 1. (Color online) Structure of the magnetotunneling junctions is Ru(5 nm)/Cu(10 nm)/Ru(5 nm)/IrMn(10 nm)/CoFeB(4 nm)/Al(1.2 nm)-oxide/CoFeB(4 nm)/Ru(5 nm) and equivalent circuit with contributions from magnetotunneling junctions.

^{a)} Author to whom correspondence should be addressed; electronic mail: ydyao@phys.sinica.edu.tw

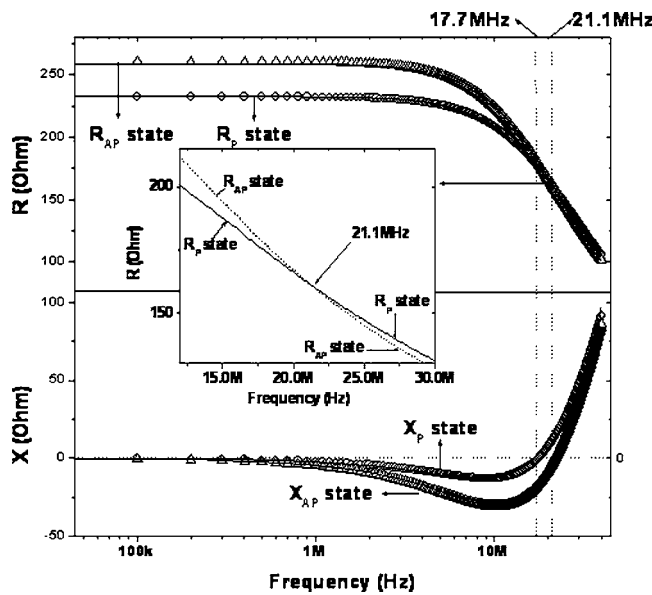


FIG. 2. Frequency dependences of the real part of the impedance (R) and the imaginary part of impedance (X) for the magnetotunneling junctions in the parallel and antiparallel states. The inset panel shows the crossover frequency of the real part of the impedance, which indicates that the magnetic behavior of MTJ is changed by the driving frequency.

circuit (EC) theory could be used to analyze our sample. The EC consists of two parts, the MTJ and the sensing circuit, as sketched in Fig. 1. In the MTJ part, the circuit contains not only the resistance (R_{barrier}) and capacitance (C_{barrier}) from the barrier but also has contributions from the interfaces, R_{int} and C_{int} , respectively. In the other part, the circuit components contain a resistor, a capacitor, and an ignorable inductor; however, this part does not respond to the variation of the magnetic field. According to the EC theory, $Z=R_{\text{eff}}+iX_{\text{eff}}$ can be expressed as follows:

$$R_{\text{eff}} = R_{\text{barrier}} / \{ [1 + (2\pi f C_{\text{barrier}} R_{\text{barrier}})^2] \} + R_{\text{int}} / \{ [1 + (2\pi f C_{\text{int}} R_{\text{int}})^2] \} + R_{\text{wire}} + R_{\text{wire-1}} / \{ [1 + (2\pi f C_{\text{wire}} R_{\text{wire-1}})^2] \}, \quad (1)$$

$$X_{\text{eff}} = 2\pi f \{ L_{\text{wire}} - C_{\text{barrier}} R_{\text{barrier}}^2 / [1 + (2\pi f C_{\text{barrier}} R_{\text{barrier}})^2] - C_{\text{int}} R_{\text{int}}^2 / [1 + (2\pi f C_{\text{int}} R_{\text{int}})^2] - C_{\text{wire}} R_{\text{wire-1}}^2 / [1 + (2\pi f C_{\text{wire}} R_{\text{wire-1}})^2] \}. \quad (2)$$

The solid line of these equations as a function of frequency is displayed in Fig. 2, which shows good agreement with experimental results (dot). The simulated values of R_{barrier} , R_{int} , C_{barrier} , and C_{int} in the parallel state are found to be 155.75 Ω , 83.60 Ω , 54.21 pF, and 38.16 pF, respectively, and those of R_{barrier} , R_{int} , C_{barrier} , and C_{int} in the antiparallel state are 204.82 Ω , 69.37 Ω , 45.35 pF, and 43.45 pF, respectively. On closer inspection of the real part of the impedance value at the crossover frequency of 21.1 MHz, as shown in the inset panel, it emerges that the real part of the impedance in the parallel state is equal to that in the antiparallel state, and after the crossover frequency, the real part of the impedance in the parallel state is larger than that in the antiparallel state. This is due to the different frequency dependences of the resistance and capacitance of the MTJ in the parallel and antiparallel states. Therefore, with an ac in MTJ, the mag-

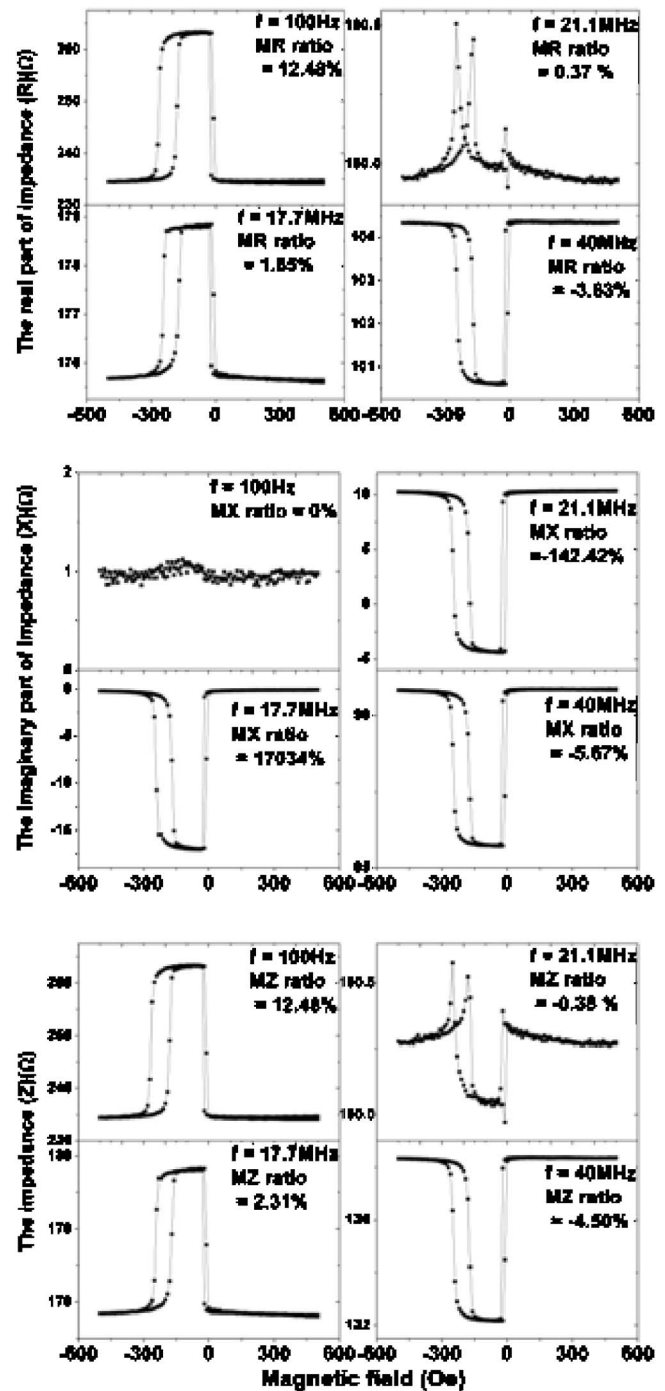


FIG. 3. (a) Real part of the impedance (R) curves at frequencies of 100 Hz, 17.7 MHz (resonance frequency), 21.1 MHz (crossover frequency), and 40 MHz for the magnetotunneling junctions. (b) The imaginary part of the impedance (X) curves at frequencies of 100 Hz, 17.7 MHz (resonance frequency), 21.1 MHz (crossover frequency), and 40 MHz for the magnetotunneling junctions. (c) The impedance (Z) curves at frequencies of 100 Hz, 17.7 MHz (resonance frequency), 21.1 MHz (crossover frequency), and 40 MHz for the magnetotunneling junctions.

netic behavior can be switched by the driving frequency. The imaginary part of the impedance of the MTJ in the parallel state X_p shows zero at a resonance frequency (f_r) of 17.7 MHz. This means that the reactance effect is zero at the resonance frequency in the parallel state, but the reactance effect of the MTJ in the antiparallel state at 17.7 MHz is not zero. According to the ratio calculation, it must have a high reactance ratio at 17.7 MHz. Therefore, we tried to take the hysteresis plots of R , X , and Z of MTJ at the interesting frequencies.

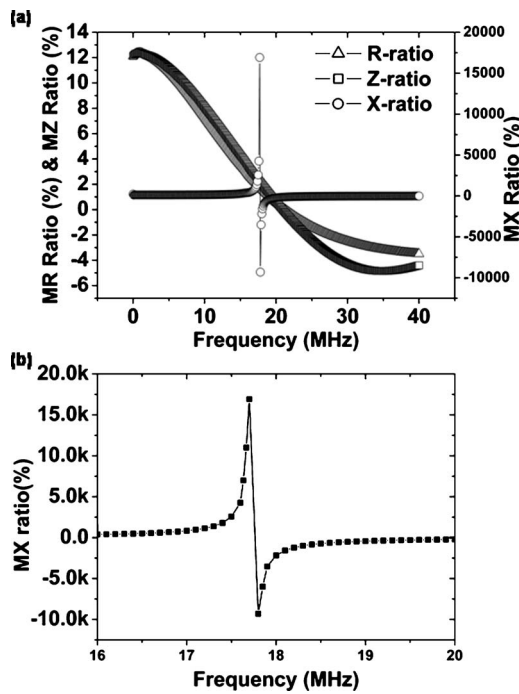


FIG. 4. (a) Frequency dependences of MR, MX, and MZ ratios. (b) The zoom in panel of the MX ratio changed; the frequency ranges from 16 to 20 MHz.

Figures 3(a)–3(c) show the real part (R), imaginary parts (X), and total impedance (Z) of the tunneling magnetoimpedance at frequencies of 100 Hz, 17.7 MHz, 21.1 MHz, and 40 MHz, respectively. The real part of the impedance decreases from 12.48% at 100 Hz to 1.85% at 17.7 MHz. It is very small (0.37%) at a frequency of 21.1 MHz, and the MR ratio changes signs after crossing the 21.1 MHz line. The MR ratio becomes -3.63% at 40 MHz, as shown in Fig. 3(a). The frequency dependent inverse behavior in the MR loop around a certain frequency is due to the competition among R and C parallel modes in the circuit. At a low frequency ($f < 21.1$ MHz), the effective impedance in this model, Z_R is smaller than Z_C , the R dominates, and most of the current goes through the R circuit. On the contrary, at a higher frequency ($f > 21.1$ MHz), Z_R is larger than Z_C , so the C dominates, and the reverse MR loop occurs. The imaginary part of the impedance exhibits the maximum value in its parallel state and the minimum value in its antiparallel state at frequencies of 17.7, 21.1, and 40 MHz, as shown in Fig. 3(b). The trend of the MX loop is mainly the capacitance effect in the MTJ. The capacitance is larger in the parallel state and smaller in the antiparallel state.^{9–11} The magnetoimpedance MX shows maximum and minimum values of $\pm 17\,000\%$ near a frequency of 17.7 MHz. This is due to the fact that the imaginary part of the impedance crosses zero at this resonance frequency. The frequency dependence by the total magnetoimpedance effect MZ loop is similar to that of the MR loop behavior, as shown in Fig. 3(c). $MZ = MR + iMX$, and the MR loop reverses the shape while crossing the crossover frequency of 21.1 MHz. Consequently, MZ reverses its shape with quite similar behavior of the MR. Apparently, Fig. 3 shows that the magnetization reversal depends on the driving frequency of the sensing current. However, this is not true, as shown by a careful examination by magneto-optical Kerr effect (MOKE) measurements, since the hysteresis loops extracted by MOKE at the same time of MI measure-

ments did not show any difference at different frequencies even around the f_r .

The frequency dependences of the MZ, MR, and MX ratios are shown in Fig. 4(a). The ratios of MZ and MR at 100 Hz are close to 13%. As the frequency increases, the MZ and MR ratio decreases, approaching zero near 21.1 MHz. This is due to the difference between the parallel and antiparallel states of Z and R being diminished as the frequency increases. However, beyond the crossover frequency (21.1 MHz), the MZ and MR ratios change their signs and become negative values, as shown in Fig. 4(a). The MX ratio shows a divergent behavior at the resonance frequency (17.7 MHz). The value of the MX ratio is small at frequencies farther away from this resonance frequency, since the value of X_p is very close to zero and changes its sign at the resonance frequency. Therefore, a small change in X_{AP} would bring about a great change in the MX ratio ($\sim 17\,000\%$ in the present sample). The MX ratio changes the sign near the resonance frequency, as shown in Fig. 4(b).

In summary, the ac behavior in a magnetic tunneling junction has been studied. We observed a huge enhancement of magnetoimpedance and an inverted MZ loop in a MTJ system. The MTJ can be regarded as a combination of resistances (R_{barrier} , R_{int} , R_{wire} , $R_{\text{wire-1}}$), inductances (L_{wire}), and capacitances (C_{barrier} , C_{int} , C_{wire}), and equivalent circuit theory can be used to analyze the ac behaviors of this system. The vanishing point of X_p was found near the resonance frequency f_r , 17.7 MHz. The MX ratio changes its sign from negative at $f < f_r$ to positive at $f > f_r$ of the frequency dependence behavior. A huge change of more than $\pm 17\,000\%$ has been observed in the imaginary part of the impedance between the magnetically parallel and antiparallel states of the MTJ. Furthermore, the inverse behavior of the magnetoimpedance loop occurs near 21.1 MHz, which is due to the crossover effect of the magnetocapacitance between magnetically parallel and antiparallel states. Our study suggests that MTJ is potentially a sensitive sensor for high frequencies.

The authors would like to thank the financial support by the Nano-research project between Academia Sinica and Industrial Technology Research Institute, and by the ROC MOEA and NSC under Grant Nos. 5301-(XS4210&XSY240) and 95-2112-M-001-059, respectively.

¹J. M. George, L. G. Pereira, A. Barthélemy, F. Petroff, L. Steren, J. L. Duvail, A. Fert, R. Loloee, P. Holody, and P. A. Schroeder, *Phys. Rev. Lett.* **72**, 408 (1994).

²J. S. Moodera, L. R. Kinder, T. M. Wong, and R. Meservey, *Phys. Rev. Lett.* **74**, 3273 (1995).

³J. M. De Teresa, A. Barthélemy, A. Fert, J. P. Contour, F. Montaigne, and P. Senor, *Science* **286**, 507 (1999).

⁴Zhong-Ming Zeng, Xiu-Feng Han, Wen-Shan Zhan, Yong Wang, Ze Zhang, and Shufeng Zhang, *Phys. Rev. B* **72**, 054419 (2005).

⁵M. F. Gillies, A. E. T. Kuiper, R. Coehoorn, and J. J. T. M. Donkers, *J. Appl. Phys.* **88**, 429 (2000).

⁶J. C. A. Huang and H. S. Hsu, *Appl. Phys. Lett.* **87**, 132503 (2005).

⁷K. Okada and T. Sekino, *Impedance Measurement Handbook* (Agilent Technologies, Santa Clara, CA, 2003).

⁸M. F. Gillies, A. E. T. Kuiper, R. Coehoorn, and J. J. T. M. Donkers, *J. Appl. Phys.* **88**, 429 (2000).

⁹H. Kaiju, S. Fujita, T. Morozumi, and K. Shiiki, *J. Appl. Phys.* **91**, 7430 (2002).

¹⁰T. Y. Peng, S. Y. Chen, L. C. Hsieh, C. K. Lo, Y. W. Huang, W. C. Chien, and Y. D. Yao, *J. Appl. Phys.* **99**, 08H710 (2006).

¹¹W. C. Chien, T. Y. Peng, L. C. Hsieh, C. K. Lo, and Y. D. Yao, *IEEE Trans. Magn.* **42**, 2624 (2006).